Communications in Information and Systems
Volume 22, Number 1, 131–146, 2022

FC-NURBS curves: fullness control non-uniform rational B-spline curves

Chongyang Deng*, Zhihao Wang†, Jianzhen Liu‡, Huixia Xu§, and Qianqian Hu¶

We present an approach to design non-uniform rational B-spline (NURBS) curves with fullness control and name the resulting curves as FC-NURBS curves. Given a point sequence and associated fullness parameters, firstly we construct a rational quadratic Bézier curve based on each adjacent three points and the fullness parameter of the middle point. Then using de Casteljau algorithm we divide each rational Bézier curve into two halves. Finally, all these halves are used to construct a C^m continuous FC-NURBS curve by combining rational polynomial blending functions. Each segment of FC-NURBS curves is a rational polynomial curve, and thus FC-NURBS curves can be converted to NURBS curves exactly. Each end segment of FC-NURBS curve is defined by neighboring three points in the point sequence and the fullness parameter of the middle point, and each non-end segment is ruled by adjacent four points in the point sequence and the fullness parameters of the two interior points. The fullness parameters, determining the proximity between the curve and corresponding points, effectively improve the local shape control ability of FC-NURBS curves. Some numerical examples are further offered to demonstrate the efficiency of our approach.

*Research supported by the National Natural Science Foundation of China (No. 61872121), and the Zhejiang Provincial Science and Technology Program in China (No. 2021C01108).

†Research supported by the National Natural Science Foundation of China (No. 61872121).

‡Research supported by the Natural Science Foundation of Zhejiang Province (No. LQ17A010009).

§(Corresponding author) Research supported by the Ningbo Natural Science Foundation (No. 2019A610033).

¶Research supported by the Natural Science Foundation of Zhejiang Province (No. LY19F020004).

1. Introduction

Shape design of free-form parametric curves and surfaces plays a fundamental role in CAGD and related fields [1, 2]. To acquire the easiness and flexibility of shape editing, curves and surfaces constructed by control points associated with various kinds of basis functions have been widely investigated.

In this paper we provide fullness control non-uniform rational B-spline curves (FC-NURBS curves), which are defined by control points associated with blending functions. The control points are obtained by de Casteljau algorithm from rational quadratic Bézier curves with fullness parameters. Our approach concentrates on the local control ability and accurate conversion into NURBS curves. Under this background, the comparison with NURBS curves and P-curves are made from the influence regions caused by the change of fullness parameters and control points.

NURBS curves and surfaces are the most popular approaches because of their universality, nice properties and incorporation in international standards such as STEP [3]. Nevertheless, the support region of NURBS basis functions is related to their degree and so high degree NURBS curves are not very local. On the other hand, the effect of the weights of NURBS curves is not clear.

P-curves, proposed by Kovács and Várady [4], are defined by control polygon associated with new basis functions inspired by the mean value generalized barycentric coordinates. The fullness parameter globally adjusts the proximity between the curve and its control polygon. In 2018, the same authors [5] use square roots of polynomials and shape parameters to create new types of curves and surfaces representation called P-Bézier curves and P-Bspline curves. The shape parameter is beneficial to globally modify the curve and relevant control polygon which helps adjust the sensitivity for the control points.

Inspired by the concept of fullness control and for purpose of designing curves being compatible with NURBS curves, we offer a new representation called FC-NURBS curves. The interdependent curve properties of designed curves are described by the fullness parameters. When the fullness parameter becomes larger, the curve runs close to the control polygon and the corresponding control points have stronger effect on the curves. Compared with NURBS curves and P-curves, less influence regions are affected no matter the change of fullness parameters or control points. In addition, the proposed curves provide more interesting properties, including positive basis functions with partition of unity, maintaining C^m end constraints and precisely shifting to NURBS curves.

The rest of this paper is organized as follows. In Section 2 we briefly introduce the related work and Section 3 proposes the construction procedure and definition of our fullness control curves. Then in Section 4 we prove the C^m continuous property and analyse the shape properties of FC-NURBS curves. Some numerical examples are furnished to illustrate the advantages of our approach in Section 5. At last, we make conclusions in Section 6.

2. Related work

In the last few decades, many researchers have shown great interests in the representation of parametric curves and surfaces, and lots of publications have been published based on different kinds of basis functions and alternatives to better control the shape. In this paper we will intensively introduce the classical literatures in the late seventies and eighties and those in recent publications.

Bézier curves are defined by the famous Bernstein polynomials with C^∞ continuity for the whole curve segment [1, 2]. In order to locally adjust the shape of the curve, B-spline curves have been generalized [6–8]. Afterwards, NURBS curves are developed not only to inherit the geometric properties of B-spline curves, but also to precisely represent the conic curves [1, 9]. When we decrease the value of one weight of a degree k NURBS curve, the shape will be dragged out of the location of the corresponding control point and $k+1$ curve segments of NURBS curves will be affected. Consequently, if the degree of the NURBS curve goes higher and higher, the influence regions of whole NURBS curves will become much larger.

In addition to aboved approaches directed at recommending additional fullness parameters for local modification, there are a number of papers introducing different kinds of basis functions to obtain extra freedom for shape design. Zhang [10] presents the trigonometric variants of the Bernstein polynomials. Combining with shape parameters, Han [11] and Han [12] develop quadratic and cubic trigonometric polynomial curves respectively. Zhu et al. [13] combines a fairly complex degree elevation algorithm to generate CB-spline curves. Brilleaud and Mazure [14] mix hyperbolic space with trigonometric space to define the basis functions for shape design. Chen [15] presents quasi-Bézier curves with several fullness parameters. Goldman and Simeonov [16] utilizes quantum calculus to modify Bernstein polynomials.

In 2017, Kovács and Várady [4] define P-curves which are proximity curves. This kind of curves have positive basis functions with partition of unity, internal C^∞ continuity and G^1 endpoint constraints. Moreover, when the fullness parameter is modified, the proximity between the curve and the control polygon would globally change. Afterwards, Kovács and Várady [5] further propose some other new proximity curves called P-Bézier curves and P-Bspline curves. The basis functions of those curves are calculated by a much simple algebra contributing to generating normal formulations like Bézier and B-spline curves and the designed curves guarantee C^m end constraints. An interesting operation guarantees that the control point insertion preserves the curve and control polygon as well.

In this paper, we will introduce a different proximity scheme called FC-NURBS curves whose control points are constructed from rational quadratic Bézier curves with de Casteljau algorithm. The constructed FC-NURBS curves are compatible with NURBS curves, C^m end constraints and locally adjust the distance between the curve and the control polygon with the fullness parameters. When one fullness parameter is altered, only two relevant curve segments are affected which is less than influenced regions of NURBS curves and P-curves.

3. Construction of FC-NURBS curves

Let the point sequence and fullness parameters be $\{\mathbf{P}_0, \mathbf{P}_1, \cdots, \mathbf{P}_n\}$ and $\{w_1, w_2, \cdots, w_{n-1}\}$ $(w_i > 1,\ i = 1, 2, ..., n-1)$, respectively. Firstly we construct $n-1$ rational quadratic Bézier curves $\mathbf{S}_i(t)$ $(i = 1, 2, \cdots, n-1)$ as follows (see Fig. 1(a)).

$$\mathbf{S}_i(t) = \frac{(1-t)^2\mathbf{P}_{i-1} + 2(1-t)tw_i\mathbf{P}_i + t^2\mathbf{P}_{i+1}}{(1-t)^2 + 2(1-t)tw_i + t^2}, t \in [0,1]. \tag{1}$$

From

$$\mathbf{P}_i - \mathbf{S}_i\left(\frac{1}{2}\right) = \frac{1}{1+w_i}\left(\mathbf{P}_i - \frac{\mathbf{P}_{i-1} + \mathbf{P}_{i+1}}{2}\right),$$

we find that the distance from $\mathbf{P}_i$ to $\mathbf{S}_i(\frac{1}{2})$ can be adjusted by the fullness parameter w_i: the bigger the w_i, the smaller the distance between $\mathbf{P}_i$ and $\mathbf{S}_i(\frac{1}{2})$, and vice versa.

Secondly, using de Casteljau algorithm we split each curve $\mathbf{S}_i(t)$ at $\mathbf{S}_i\left(\frac{1}{2}\right)$ into two rational quadratic Bézier curves $\mathbf{S}_{i,1}(t), \mathbf{S}_{i,2}(t)$, $i = 1, 2, \cdots, n-1$, (see Fig. 1(b))

$$\mathbf{S}_{i,1}(t) = \frac{(1-t)^2\mathbf{Q}_{i,0} + 2(1-t)t\overline{w}_i\mathbf{Q}_{i,1} + t^2\overline{w}_i\mathbf{Q}_{i,2}}{(1-t)^2 + 2(1-t)t\overline{w}_i + t^2\overline{w}_i}, t \in [0,1], \tag{2}$$

$$\mathbf{S}_{i,2}(t) = \frac{(1-t)^2\overline{w}_i\mathbf{R}_{i,0} + 2(1-t)t\overline{w}_i\mathbf{R}_{i,1} + t^2\mathbf{R}_{i,2}}{(1-t)^2\overline{w}_i + 2(1-t)t\overline{w}_i + t^2}, t \in [0,1], \tag{3}$$

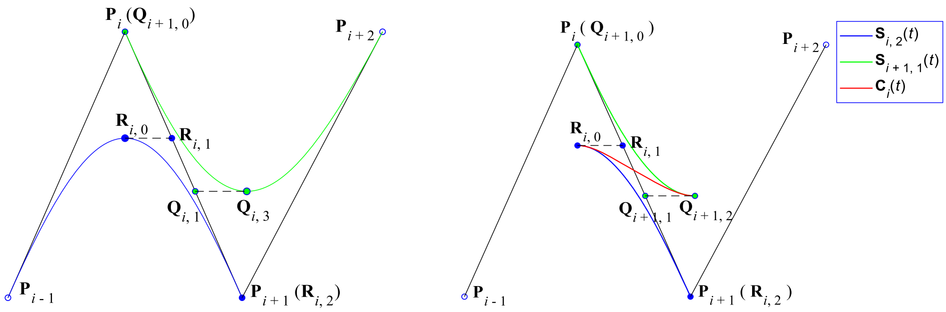

(a) (b)

Figure 1: **(a)**: the generation of points $\mathbf{Q}_{i+1,0}, \mathbf{Q}_{i+1,1}, \mathbf{Q}_{i+1,2}$ and $\mathbf{R}_{i,0}, \mathbf{R}_{i,1}, \mathbf{R}_{i,2}$; **(b)**: the construction of two rational quadratic curves $\mathbf{S}_{i+1,1}(t), \mathbf{S}_{i,2}(t)$ and the curve segments $\mathbf{C}_i(t), i = 1, 2, \cdots, n-2$.

where

$$\overline{w}_i = \frac{1+w_i}{2};$$

$$\mathbf{Q}_{i,0} = \mathbf{P}_{i-1}, \ \mathbf{Q}_{i,1} = \frac{w_i \mathbf{P}_i + \mathbf{P}_{i-1}}{1+w_i}, \ \mathbf{Q}_{i,2} = \frac{\mathbf{P}_{i-1} + 2w_i \mathbf{P}_i + \mathbf{P}_{i+1}}{2+2w_i};$$

$$\mathbf{R}_{i,0} = \frac{\mathbf{P}_{i-1} + 2w_i \mathbf{P}_i + \mathbf{P}_{i+1}}{2+2w_i}, \ \mathbf{R}_{i,1} = \frac{w_i \mathbf{P}_i + \mathbf{P}_{i+1}}{1+w_i}, \ \mathbf{R}_{i,2} = \mathbf{P}_{i+1}.$$

Now, each edge of $\{\mathbf{P}_i \mathbf{P}_{i+1}\}_{i=1}^{n-2}$ corresponds to two rational quadratic curves $\mathbf{S}_{i+1,1}(t)$ and $\mathbf{S}_{i,2}(t)$, while edges $\mathbf{P}_0\mathbf{P}_1, \mathbf{P}_{n-1}\mathbf{P}_n$ correspond to rational quadratic curves, $\mathbf{S}_{1,1}(t), \mathbf{S}_{n-1,2}(t)$, respectively.

Thirdly, combining blending functions

$$F_{i,m}(t) = \frac{t^{m+1}}{(1-t)^{m+1} + t^{m+1}}, \tag{4}$$

$$G_{i,m}(t) = 1 - F_{i,m}(t) = \frac{(1-t)^{m+1}}{(1-t)^{m+1} + t^{m+1}}, \tag{5}$$

with $\mathbf{S}_{i+1,1}(t), \mathbf{S}_{i,2}(t)$ we define curve segments as (see Fig. 1(b))

$$\begin{aligned} \mathbf{C}_i(t) &= F_{i,m}(t)\mathbf{S}_{i+1,1}(t) + G_{i,m}(t)\mathbf{S}_{i,2}(t), \\ & t \in [0,1], \ i = 1, 2, \cdots, n-2. \end{aligned} \tag{6}$$

The first and last curve segments $\mathbf{C}_0(t)$ and $\mathbf{C}_{n-1}(t)$ are defined by (see

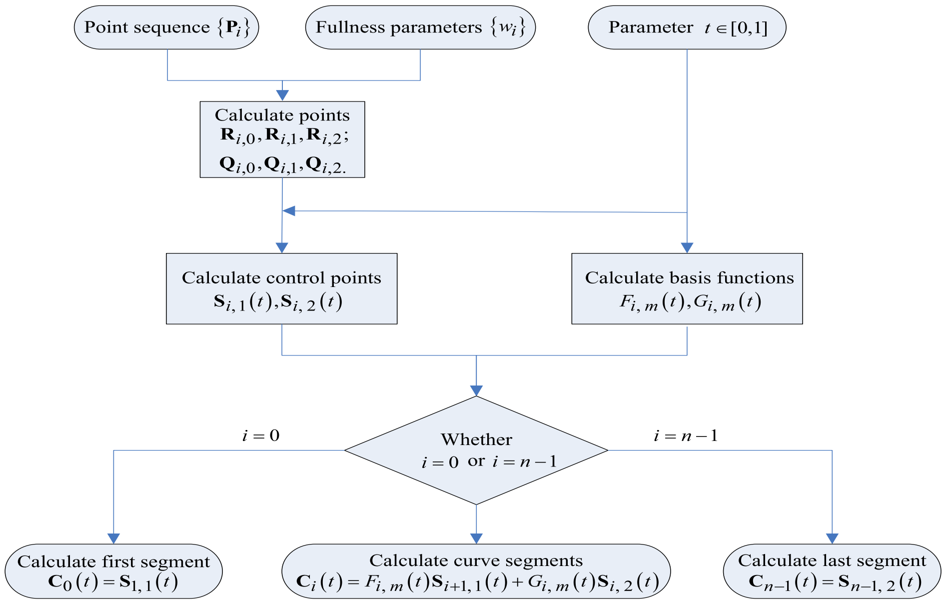

Figure 2: Flow chart of our scheme.

Fig. 1(b))

(7) $$\mathbf{C}_0(t) = \mathbf{S}_{1,1}(t),\ \mathbf{C}_{n-1}(t) = \mathbf{S}_{n-1,2}(t),\ t \in [0,1].$$

Finally, we get a sequence of curve segments $\{\mathbf{C}_i(t)\}_{i=0}^{n-1}$ and we will prove that they are C^m continuous at their joints. Each segment $\mathbf{C}_i(t)$ is a rational polynomial curve and accordingly the resulting whole curve $\mathbf{C}(t) = \{\mathbf{C}_i(t)\}_{i=0}^{n-1}$ can be transformed into a NURBS curve. Furthermore, $\mathbf{C}_i(t)$ can be modulated by fullness parameters, so we denominate the resulting curve $\mathbf{C}(t) = \{\mathbf{C}_i(t)\}_{i=0}^{n-1}$ as FC-NURBS curve.

Following Fig. 2 further depicts the process of our construction scheme.

Remark 1. If the parameter w_i is too small, the distance between the control point $\mathbf{P}_i$ and the devised curve is very far and then the shape of the curve is very poor. Therefore, all the fullness parameters are set in advance satisfying $w_i > 1$ $(i = 1, 2, \cdots, n-1)$.

4. Properties of FC-NURBS curves

In this section we will prove the continuous properties of FC-NURBS curves and analyze their shape characters.

4.1. Continuity

This subsection will demonstrate that the designed curve is C^m continuous at $t=0$ in each curve segment $\mathbf{C}_i(t)$ or $t=1$ in curve segment $\mathbf{C}_{i-1}(t)$ $(i=1,2,\cdots,n-1)$. In order to prove the property, we firstly present a lemma about the blending functions.

Lemma 2. *For the blending functions $F_{i,m}(t), G_{i,m}(t)$, we have*

$$\begin{aligned}
&F_{i,m}(0)=0,\ \ G_{i,m}(0)=1,\\
&\frac{d^kF_{i,m}(0^+)}{dt^k}=\frac{d^kG_{i,m}(0^+)}{dt^k}=0,\ \ k=1,2,\cdots,m;
\end{aligned}\tag{8}$$

$$\begin{aligned}
&F_{i-1,m}(1)=1,\ \ G_{i-1,m}(1)=0,\\
&\frac{d^kF_{i-1,m}(1^-)}{dt^k}=\frac{d^kG_{i-1,m}(1^-)}{dt^k}=0,\ \ k=1,2,\cdots,m.
\end{aligned}\tag{9}$$

Here $\frac{d^kF_{i,m}(0^+)}{dt^k}$, $\frac{d^kG_{i,m}(0^+)}{dt^k}$ are k-order right derivatives of $F_{i,m}(t)$, $G_{i,m}(t)$ at $t=0$, and $\frac{d^kF_{i-1,m}(1^-)}{dt^k}$, $\frac{d^kG_{i-1,m}(1^-)}{dt^k}$ are k-order left derivatives of $F_{i-1,m}(t)$, $G_{i-1,m}(t)$ at $t=1$.

Proof. We will verify the lemma from four cases as follows.

(I) From (7) we know that when $t\in[0,1]$ in the first curve segment $\mathbf{C}_0(t)$, all $F_{0,m}(t)=1$ and $G_{0,m}(t)=0$ hold. Therefore, all $\frac{d^kF_{0,m}(1^-)}{dt^k}=\frac{d^kG_{0,m}(1^-)}{dt^k}=0$ establish for $k=1,2,\cdots,m$.

(II) As can be seen from (7), all $F_{n-1,m}(t)=0$ and $G_{n-1,m}(t)=1$ are set up in the last curve segment $\mathbf{C}_{n-1}(t)$ when $t\in[0,1]$. Hence, every $\frac{d^kF_{n-1,m}(0^+)}{dt^k}=\frac{d^kG_{n-1,m}(0^+)}{dt^k}=0$ hold, $k=1,2,\cdots,m$.

(III) When t equals 0 in the intermediate curve segment $\mathbf{C}_i(t)$ $(i=1,2,\cdots,n-2)$, we get $F_{i,m}(0)=0$ and $G_{i,m}(0)=1$. Next step is to prove $\frac{d^kF_{i,m}(0^+)}{dt^k}=\frac{d^kG_{i,m}(0^+)}{dt^k}=0$ by mathematical induction.

For $k=1$, due to $F_{i,m}(t)$ is a rational function in t, we find that $\frac{dF_{i,m}(t)}{dt}$ is still a rational function in t. In addition, the denominator of $\frac{dF_{i,m}(t)}{dt}$ is unequal to zero, so $\frac{dF_{i,m}(t)}{dt}$ is right continuous at $t=0$ in the segment $\mathbf{C}_i(t)$ $(i=1,2,\cdots,n-2)$. Then with L'Hospital's rule we have

$$\begin{aligned}
\frac{dF_{i,m}(0^+)}{dt}&=\lim_{t\to0^+}\frac{F_{i,m}(t)-F_{i,m}(0)}{t}=\lim_{t\to0^+}\frac{F_{i,m}(t)}{t}\\
&=\lim_{t\to0^+}\frac{dF_{i,m}(t)}{dt}=\frac{dF_{i,m}(t)}{dt}\Big|_{t=0}.
\end{aligned}$$

Furthermore, the product factor t^m is included in $\frac{dF_{i,m}(t)}{dt}$. Therefore with the equality $G_{i,m}(t) = 1 - F_{i,m}(t)$ we find that

$$\frac{dF_{i,m}(0^+)}{dt} = \frac{dG_{i,m}(0^+)}{dt} = 0.$$

By induction, we assume for arbitrary positive integer $m-1$, the conclusion $\frac{d^{m-1}F_{i,m}(0^+)}{dt^{m-1}} = 0$ is true. After differentiate m times, $\frac{d^m F_{i,m}(t)}{dt^m}$ is still a rational function in t. As a result, $\frac{d^m F_{i,m}(t)}{dt^m}$ is right continuous at $t = 0$. Continuing with L'Hospital's rule, we derive m derivative from the assumption:

$$\begin{aligned}\frac{d^m F_{i,m}(0^+)}{dt^m} &= \lim_{t\to 0^+} \frac{\frac{d^{m-1}F_{i,m}(t)}{dt^{m-1}} - \frac{d^{m-1}F_{i,m}(0^+)}{dt^{m-1}}}{t} \\ &= \lim_{t\to 0^+} \frac{d^m F_{i,m}(t)}{dt^m} = \frac{d^m F_{i,m}(t)}{dt^m}\Big|_{t=0}.\end{aligned}$$

Together with the fact that $\frac{d^m F_{i,m}(t)}{dt^m}$ contains the product factor t and the equality $G_{i,m}(t) = 1 - F_{i,m}(t)$ holds, we find the following equalities:

$$\frac{d^m F_{i,m}(0^+)}{dt^m} = \frac{d^m G_{i,m}(0^+)}{dt^m} = 0,$$

which exactly means the conclusion is true when k is m. So the equality (8) follows.

(IV) For $t = 1$ in the segment $\mathbf{C}_{i-1}(t)$ $(i = 2, 3, \cdots, n-1)$, the equality (9) can be proved in a similar fashion to **Case (III)**, due to the fact that $\frac{d^k G_{i-1,m}(t)}{dt^k}$ is a rational function in $1-t$ and the product factor $(1-t)^{m+1-k}$ is involved in $\frac{d^k G_{i-1,m}(t)}{dt^k}$ $(k = 1, 2, \cdots, m)$.

On the ground of aforesaid analyses, it can be found that (8) and (9) are right. □

Now we will introduce our main results.

Theorem 3. *The curve $\{\mathbf{C}_i(t)\}_{i=0}^{n-1}$ defined by (6) and (7) is C^m continuous at $t = 0$ in each curve segment $\mathbf{C}_i(t)$, or $t = 1$ in curve segment $\mathbf{C}_{i-1}(t)$, $(i = 1, 2, \cdots, n-1)$.*

Proof. From the foregoing Lemma 2, we know that

$$\begin{aligned}&F_{i-1,m}(1) = 1,\ G_{i-1,m}(1) = 0,\\ &\frac{d^k F_{i-1,m}(1^-)}{dt^k} = \frac{d^k G_{i-1,m}(1^-)}{dt^k} = 0,\ k = 1, 2, \cdots, m.\end{aligned}$$

Therefore, for the curve segment $\mathbf{C}_{i-1}(t)$ $(i = 1, 2, \cdots, n-1)$ on $t \in [0, 1]$, it can be acquired that the value of $\frac{d^k \mathbf{C}_{i-1}(1^-)}{dt^k}$ is totally decided by the value of $\frac{d^k \mathbf{S}_{i,1}(1^-)}{dt^k}$ $(k = 0, 1, \cdots, m)$. Analogously, on $t \in [0, 1]$ in each segment $\mathbf{C}_i(t)$ $(i = 1, 2, \cdots, n-1)$, the value of $\frac{d^k \mathbf{C}_i(0^+)}{dt^k}$ is equivalent to the value of $\frac{d^k \mathbf{S}_{i,2}(0^+)}{dt^k}$ $(k = 0, 1, \cdots, m)$.

According to our construction strategy, it is obvious to find that $\mathbf{S}_{i,1}(t)$ and $\mathbf{S}_{i,2}(t)$ $(i = 1, 2, \cdots, n-1)$ are located in the same rational quadratic Bézier curve, since they are acquired by subdividing the Bézier curve $\mathbf{S}_i(t)$ with de Casteljau algorithm at $\mathbf{S}_i(\frac{1}{2})$. Hence, $\mathbf{S}_{i,1}(t)$ and $\mathbf{S}_{i,2}(t)$ are C^m continuous at $t = 0$ in $\mathbf{C}_i(t)$ or $t = 1$ in $\mathbf{C}_{i-1}(t)$ $(i = 1, 2, \cdots, n-1)$, which indicates that Theorem 3 is true. $\square$

4.2. Analyses of shape properties

From the very beginning we provide the geometric characters of the fullness parameters $\{w_i\}_{i=1}^{n-1}$, then present the impact of the alteration of fullness parameters and control points on the generated curves' shape.

As can be seen from the definition of $\mathbf{R}_{i,0}$ and $\mathbf{R}_{i,1}$, these two points are getting close to the point $\mathbf{P}_i$ when the parameter w_i increases. Adding the condition $\mathbf{S}_{i,2}(0) = \mathbf{R}_{i,0}$, we find that the distance between the point $\mathbf{P}_i$ and the control point $\mathbf{S}_{i,2}(0)$ shrinks when w_i increases. Then according to the equality $\mathbf{C}_i(0) = \mathbf{S}_{i,2}(0)$, we know that w_i helps to regulate the space from the point $\mathbf{P}_i$ to the relevant curve point $\mathbf{C}_i(0)$. Similarly, the separation between the point $\mathbf{P}_i$ and the corresponding curve point $\mathbf{C}_{i-1}(1)$ expands as well when w_i decreases.

Furthermore, we will offer how the change of fullness parameters influences the shape of curves. As described above, the alteration of parameter w_i affects the value of $\mathbf{R}_{i,0}$ and $\mathbf{R}_{i,1}$, which decide the control point $\mathbf{S}_{i,2}(t)$. Meanwhile, w_i also has impact on the value of $\mathbf{Q}_{i,1}$ and $\mathbf{Q}_{i,2}$ determining the control point $\mathbf{S}_{i,1}(t)$. Consequently, the fullness parameter w_i will have influence on the shape of two curve segments $\mathbf{C}_{i-1}(t)$ and $\mathbf{C}_i(t)$.

One more thing, the change of one point $\mathbf{P}_i$ will have influence on the form of four curve segments containing $\mathbf{C}_{i-2}(t)$, $\mathbf{C}_{i-1}(t)$, $\mathbf{C}_i(t)$ and $\mathbf{C}_{i+1}(t)$. It is because that when we alter the position of the point $\mathbf{P}_i$, the values of control points $\{\mathbf{S}_{j,1}(t)\}_{j=i-1}^{i+1}$ and $\{\mathbf{S}_{j,2}(t)\}_{j=i-1}^{i+1}$ will be altered. Consequently, the corresponding four curve segments will change their shape.

5. Numerical examples and comparisons

In this section, we will provide some numerical examples to show the efficiency of our approach. Of all graphs, polygons and their corresponding generated curves are identified with black line segments and colorful curves respectively.

Example 4. Two convex polygons and their generated C^2 and C^3 curves, defined on $t \in [0, 1]$, are presented in Fig. 3. Initial vertices of the convex polygon in Fig. 3(a) are $(5, 1)$, $(2, 3)$, $(2, 8)$, $(6, 10)$, $(10, 8)$, $(10, 3)$ and $(7, 1)$, and original control points of the convex polygon in Fig. 3(b) are $(-2.17, 5.64)$, $(-11.75, 3.4)$, $(-12, 2)$, $(-6.83, -4.23)$, $(-5.2, -4)$ and $(0.77, 4)$.

Fig. 3 also provides two concave polygons and their generated C^2 and C^3 curves defined on $t \in [0, 1]$. In Fig. 3(c), the points of the concave polygon are $(9.24, 8.35)$, $(7.24, 9.8)$, $(4.76, 9.8)$, $(2.76, 8.35)$, $(6, 6)$, $(2.76, 3.65)$, $(4.76, 2.2)$, $(7.24, 2.2)$, $(9.24, 3.65)$ and $(10, 6)$. In Fig. 3(d), the original vertices are $(-9.8, 2.9)$, $(-5.7, 3.2)$, $(-4.8, 6.6)$, $(-10, 6.4)$, $(-11.3, 1.6)$, $(-7.3, -1.5)$ and $(-3.8, 1.9)$.

In Fig. 3, upper left figure offers all fullness parameters $\{w_i\}_{i=1}^5$ values 2 except for varying w_3 from 2 to 1 and 3 and upper right graph provides all fullness parameters $\{w_i\}_{i=1}^4$ values 2 except for varying w_2 from 2 to 1 and 3, creating the corresponding blue and green curves respectively. Meanwhile, lower left graph presents all fullness parameters $\{w_i\}_{i=1}^8$ values 2 except that w_4 is varied from 2 to 1 and 3 and lower right figure offers all fullness parameters $\{w_i\}_{i=1}^5$ values 2 except for varying w_5 from 2 to 1 and 3, generating the corresponding blue and green curves respectively.

As shown in Fig. 3(a), it can be found that the distance between the point $\mathbf{P}_3$ and the relevant points $\mathbf{C}_3(0)$ or $\mathbf{C}_2(1)$ (shown in blue cross) shrinks as w_3 increases. Simultaneously, when the parameter w_2 decreases, the distance from the point $\mathbf{P}_2$ to the corresponding points $\mathbf{C}_2(0)$ or $\mathbf{C}_1(1)$ (shown in blue cross) enlarges in Fig. 3(b). Moreover, the lower two figures show that this nice property similarly holds for the concave polygons.

Example 5. Fig. 4 compares the effect caused by the alteration of one parameter among quintic NURBS curves, P-curves and our FC-NURBS curves. The involved control vertices are $(3, 8)$, $(3, 4)$, $(5, 1)$, $(5, 7)$, $(7, 9)$, $(7, 2)$, $(9, 5)$, $(9, 10)$, $(11, 9)$ and $(11, 6)$. The original red NURBS curve is defined on the knot vector $[0, 0, 0, 0, 0, 0, 0.11, 0.2, 0.36, 0.44, 0.63, 0.73, 0.86, 0.92, 1, 1, 1, 1, 1, 1]$ and has all weights equivalent to 1, while only w_4 is changed by the number 5 in the blue NURBS curve. The primitive red P-curve is defined on the knot vector $[0, 0.11, 0.2, 0.36, 0.44, 0.63, 0.73, 0.86, 0.92, 1]$ and shaped with the parameter $\gamma = 0.05$, while γ is varied to 0.1 in the blue curve. Our red FC-NURBS curve assigns all fullness parameters $\{w_i\}_{i=1}^8$ the value 1.8, while only w_4 is reassigned the value 3 in the blue curve.

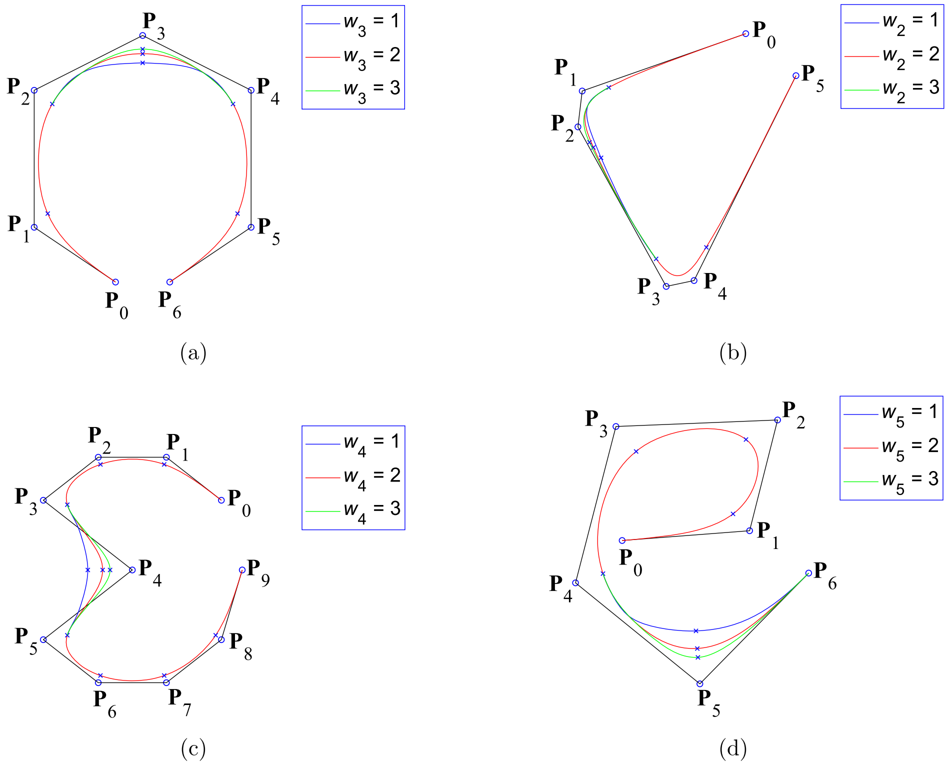

Figure 3: **(a)**: convex hexagon and created three C^2 curves; **(b)**: convex pentagon and created three C^3 curves; **(c)**: concave polygon and created three C^2 curves; **(d)**: concave polygon and created three C^3 curves.

As can be seen from Fig. 4, when only one parameter is changed, there are six curve segments affected for the quintic NURBS curves and whole curve segments influenced for P-curves, while only two curve segments are affected for FC-NURBS curves.

Example 6. The difference affected by the alteration of one control point is presented among quintic NURBS curves, P-curves and FC-NURBS curves in Fig. 5. All involved data, including the incipient vertices of the original polygons, the fullness parameters and knot vectors of red quintic NURBS curves, red P-curves and red FC-NURBS curves, are the same as those of red curves in Fig. 4. Except that the weight w_4 of the blue quintic NURBS curve is assigned the value 8. In addition, the vertex $\mathbf{P}_4$ varies from $(7, 9)$ to $(7, -5)$ to generate the cyan curves in Fig. 5.

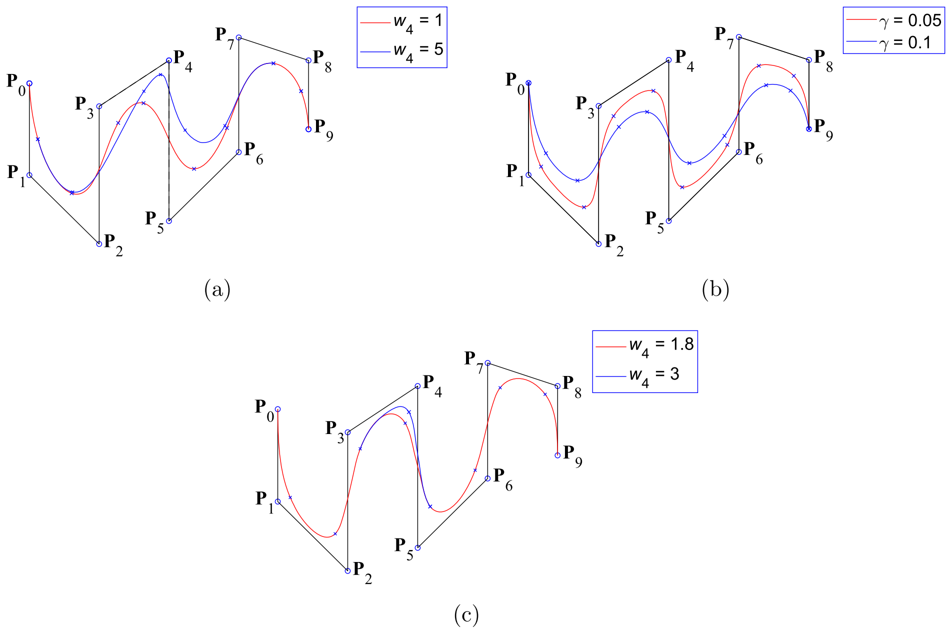

Figure 4: **(a)**: the control polygon and generated quintic C^4 NURBS curves; **(b)**: the control polygon and created C^∞ P-curves; **(c)**: the control polygon and our generated C^4 FC-NURBS curves.

From Fig. 5 we find that after alter the position of one control point, six curve segments and whole curve are influenced for quintic NURBS curves and P-curves respectively, whereas only four curve segments change their positions by our approach.

Example 7. A comparison of three kinds of curves, cubic C^2 NURBS curve, C^∞ P-curve and our C^2 FC-NURBS curve is made in Fig. 6. All concave polygons are expressed as

$$(3.52, 4.41), (0.68, 10.52), (4.88, 15.32), (8.57, 10.61), (6.58, 5.06),$$
$$(14.76, 3.80), (12.37, 6.97), (15.06, 9.87), (14.06, 15.09), (9.97, 13.04).$$

Upper cubic NURBS curve is defined on knot vector $[0, 0, 0, 0, 0.13, 0.26, 0.37, 0.49, 0.65, 0.73, 0.81, 0.91, 1, 1, 1, 1]$ and all weights are equal to 1. Middle P-curve has knot sequence $[0, 0.13, 0.26, 0.37, 0.49, 0.65, 0.73, 0.81, 0.91, 1]$ with the fullness parameter $\gamma = 0.05$. As to the lower FC-NURBS curve, all weights $\{w_i\}_{i=1}^{8}$ are 1.8.

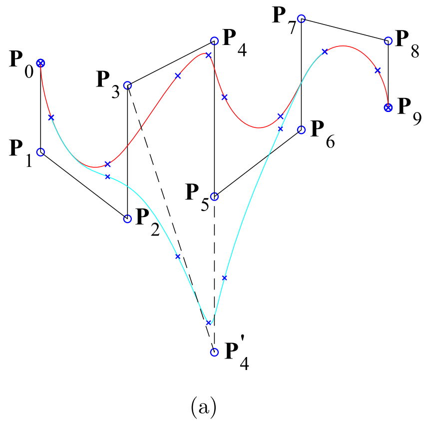

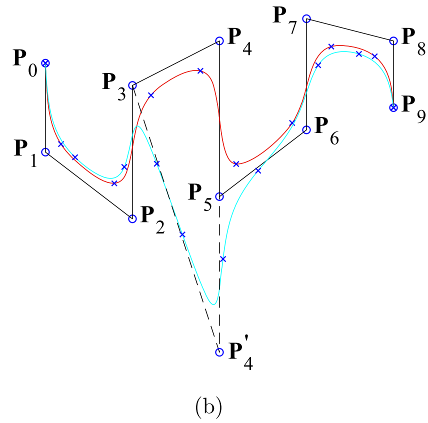

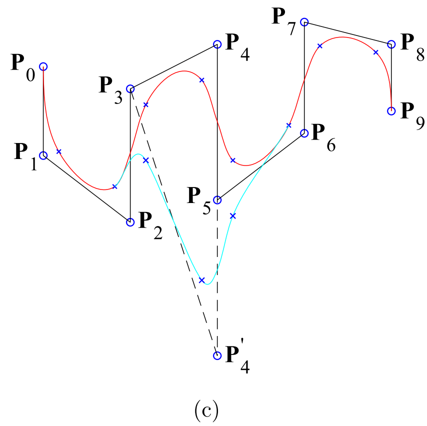

Figure 5: **(a)**: the control enneagons and generated quintic C^4 NURBS curves; **(b)**: the control enneagons and created C^∞ P-curves; **(c)**: the control polygons and our C^4 FC-NURBS curves. The cyan curves are created after altering the position of the control point $\mathbf{P}_4$ to $\mathbf{P}'_4$.

Green curves represent the curvature plots of all generated curves, which shows that our method can construct fair curves similar to cubic NURBS curves and P-curves.

6. Conclusions

We have introduced FC-NURBS curves with fullness control and local property. The fullness parameters contribute to adjusting the distances between

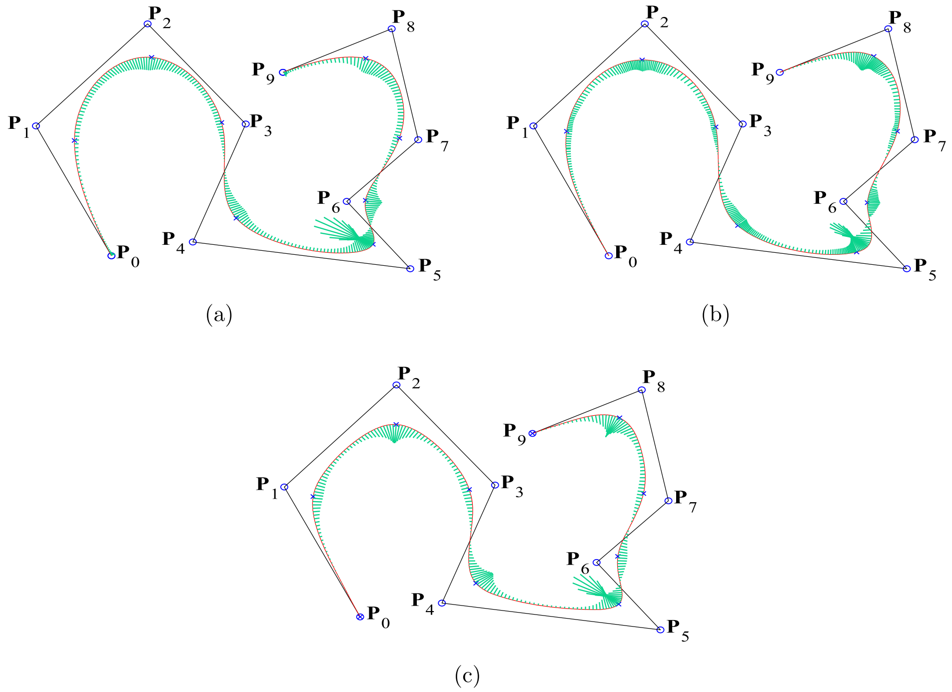

Figure 6: **(a)**: the concave polygon and generated cubic C^2 NURBS curve; **(b)**: the concave nonagon and created C^∞ P-curve; **(c)**: the concave nonagon and our C^2 FC-NURBS curve. Green curves show the curvature plot of all created three curves.

the control points and generated FC-NURBS curves. Meanwhile, the influence regions of fullness parameters in our approach are smaller than those of traditional NURBS curve and P-curve design. This verdict is appropriate for the alteration of one control point as well. Our constructed FC-NURBS curve is C^m continuous and can be converted to NURBS curve exactly. These advantages render FC-NURBS curves more room to utilize in CAGD and relevant areas.

References

[1] G. E. Farin, *Curves and surfaces for CAGD: a practical guide.* San Francisco, Morgan Kaufmann Publishers, 2002.

[2] G. J. Wang, G. Z. Wang and J. M. Zheng, *Computer aided geometric design (in Chinese)*. Beijing, China Higher Education Press; Heidelberg, Springer-Verlag, 2001.

[3] S. M. Vergeest, *CAD surface data exchange using STEP*. Computer Aided Geometric Design, **23**(4):269–281, 1991.

[4] I. Kovács and T. Várady, *P-curves and surfaces: parametric design with global fullness control*. Computer-Aided Design, **90**:113–122, 2017. MR3673566

[5] I. Kovács and T. Várady, *P-Bézier and P-Bspline curves – new representations with proximity control*. Computer Aided Geometric Design, **62**:117–132, 2018. MR3802207

[6] G. M. Nielson, *Some piecewise polynomial alternatives to splines under tension*. In "Computer Aided Geometric Design" (R. E. Barnhill and R. F. Riesenfeld eds.), pages 209–235, 1974. MR0371012

[7] B. A. Barsky and J. C. Beatty, *Local control of bias and tension in beta-splines*. ACM Transactions on Graphics, **2**(2):109–134, 1983.

[8] W. Boehm, *Curvature continuous curves and surfaces*. Computer Aided Geometric Design, **2**(4):313–323, 1985. MR0824102

[9] L. Piegl and W. Tiller, *The NURBS Book, 2nd ed.* New York, Springer, 1997.

[10] J. Zhang, *C-Bézier curves and surfaces*. Graph Models Image Process, **61**(1):2–15, 1999.

[11] X. Han, *Quadratic trigonometric polynomial curves with a shape parameter*. Computer Aided Geometric Design, **19**(7):503–512, 2002. MR1922571

[12] X. Han, *Cubic trigonometric polynomial curves with a shape parameter*. Computer Aided Geometric Design, **21**(6):535–548, 2004. MR2071821

[13] P. Zhu, G. Wang and J. Yu, *Degree elevation operator and geometric construction of CB-spline curves*. SCIENCE CHINA Information Sciences, **53**(9):1753–1764, 2010. MR2684885

[14] M. Brilleaud and M. L. Mazure, *Mixed hyperbolic/trigonometric spaces for design*. Computers δ Mathematics with Applications, **64**(8):2459–2477, 2012. MR2970827

[15] J. Chen, *Quasi-Bézier curves with shape parameters*. Journal of Applied Mathematics, **2013**:1–9, 2013. MR3039726

[16] R. Goldman and P. Simeonov, *Quantum Bernstein bases and quantum Bézier curves*. Journal of Computational and Applied Mathematics, **288**:284–303, 2015. MR3349623

Chongyang Deng
School of Science
Hangzhou Dianzi University
Hangzhou, 310018
China
E-mail address: dcy@hdu.edu.cn

Zhihao Wang
School of Science
Hangzhou Dianzi University
Hangzhou, 310018
China
E-mail address: wangzhihao1226@gmail.com

Jianzhen Liu
School of Science
Hangzhou Dianzi University
Hangzhou, 310018
China
E-mail address: ljz117@hdu.edu.cn

Huixia Xu
Institute of Mathematics
Zhejiang Wanli University
Ningbo, 315100
China
E-mail address: xuhx0916@hotmail.com

Qianqian Hu
School of Statistics and Mathematics
Zhejiang Gongshang University
Hangzhou, 310018
China
E-mail address: qianqian_hu@163.com

Received September 15, 2020